recA) carrying plasmid pRT2 was used as the host cell for screening. Plasmid pRT2 was constructed by inserting a 3.3-kb Hinc II fragment containing the *E. coli phr*$^+$ gene into the Pvu II site of pACYC184 (Bio Labs). The cDNA library was introduced into *E. coli* strain SY32 (pRT2) and incubated with 1 mM isopropylthio-β-galactoside (IPTG) for 1 hour. After plating on LB agar plates, transformed cells were exposed to 0.1 to 0.6 J/m^2 of UV light from a germicidal lamp and then illuminated for 15 min with visible light at a distance of 24 cm from a FL15D lamp (National) with a 7-mm thick soft glass filter (PR treatment). Surviving cells were collected from the plates the next day and were subjected to a second round of selection with UV plus PR treatment. After 13 rounds of selection, four single colonies were selected from the illuminated plate, and their UV sensitivity with or without PR treatment was determined. Plasmid DNA was isolated from one of the light-dependent UV-resistant colonies and designated pDm64PR.

9. T. Todo *et al.*, data not shown.
10. T. Todo *et al.*, *Mutat. Res.* **315**, 213 (1994).
11. *Drosophila* (6-4)photolyase was expressed in *E. coli* as a lacZ–α peptide fusion protein. To prepare recombinant *Drosophila* (6-4)photolyase, we incubated *E. coli* SY2 (*phr::Cm*^{r} *uvrA::Kan*^{r} *recA::Tet*^{r}) carrying pDm64PR in 150-ml cultures with 1 mM IPTG for 12 hours and then obtained lysates by sonication of bacterial pellets in sonic buffer [50 mM tris-HCl (pH 7.4), 1 mM EDTA, and 10% glycerol]. The lysates were cleared by centrifugation at 12,000*g* for 20 min. To purify protein that bound UV-irradiated DNA, we applied the cleared lysate to UV-treated DNA attached to beads. UV-DNA affinity beads were prepared as follows. Salmon sperm DNA [500 μg, previously digested with Hind III and irradiated with UV light (25 kJ/m^2)] was labeled with 500 mg of photobiotin (Vector Laboratory) by irradiation in an ice bath 10 cm below a sunlamp (Toshiba, FL20SE) with a UV-34 filter (Hoya, Tokyo). Biotin-labeled DNA was bound to streptoavidin paramagnetic beads (Promega). Approximately 400 μg of UV-irradiated DNA was bound to beads. The cleared lysates were mixed with the UV-DNA affinity beads in 1 ml of binding buffer [salmon sperm DNA (1 mg/ml), 200 mM NaCl, 50 mM tris-HCl (pH 7.4), 1 mM EDTA, and 10% glycerol]. After 15 min to allow for binding, the beads were washed twice with 1 ml of washing buffer [350 mM NaCl, 50 mM tris-HCl (pH 7.4), 1 mM EDTA, and 10% glycerol], and protein bound to the beads was eluted with 100 μl of elution buffer [1 M NaCl, 50 mM tris-HCl (pH 7.4), 1 mM EDTA, and 10% glycerol]. After repeating the elution process three times, each 100 μl of eluted solution was combined, and the resultant 300 μl of solution was used as the recombinant *Drosophila* (6-4)photolyase or control plasmid extract.
12. T. Matsunaga *et al.*, *Photochem. Photobiol.* **57**, 934 (1993).
13. A. Yasui *et al.*, *EMBO J.* **13**, 6143 (1994).
14. M. Ahmad and A. R. Cashmore, *Nature* **366**, 162 (1993).
15. K. Malhotra *et al.*, *Biochemistry* **34**, 6892 (1995).
16. S.-T. Kim *et al.*, *J. Biol. Chem.* **269**, 8535 (1994).
17. C. Lin *et al.*, *Science* **269**, 968 (1995).
18. H.-W. Park, S.-T. Kim, A. Sancar, J. Deisenhofer, *ibid.* **268**, 1866 (1995).
19. The recombinant protein migrated as a doublet of ~62 kD. The lower band may represent a degradation product.
20. A 73-bp DNA fragment enriched in the sequence TC (TC-3) was irradiated with 15 kJ/m^2 of UV light and then used in the gel shift assay.
21. The *Drosophila* (6-4)photolyase was purified from the embryo of *Drosophila phr*$^-$ strain, as in (*7*).
22. Salmon sperm DNA irradiated with UV light (8 J/m^2) and purified recombinant (6-4)photolyase were mixed in 400 μl of reaction buffer and exposed to fluorescent light for 30 min. The mixture was phenol extracted, ethanol precipitated, and used for the ELISA assay (*7*, *10*).
23. T. Kato Jr. *et al.*, *Nucleic Acids Res.* **22**, 4119 (1994).
24. K. Malhotra, S.-T. Kim, A. Sancar, *Biochemistry* **33**, 8712 (1994).
25. G. D. Small, B. Min, P. A. Lefebrre, *Plant Mol. Biol.* **28**, 443 (1995).
26. G. J. Barton and M. J. E. Sternberg, *J. Mol. Biol.* **198**, 327 (1987).
27. R. M. Schwartz and M. O. Dayhoff, in *Atlas of Protein Sequence and Structure*, M. O. Dayhoff, Ed. (National Biomedical Research Foundation, Washington, DC, 1978), pp. 353–359.
28. We thank H. Iwasaki for critical reading of the manuscript. Supported by the Grant-in-Aid for Scientific Research on Priority Areas from the Ministry of Education, Science, and Culture of Japan (numbers 05270101 and 07263240). We also thank the Integrated Molecular Analysis of Genome Expression (IMAGE) consortium for the use of their resources.

25 January 1996; accepted 5 March 1996

Silk Properties Determined by Gland-Specific Expression of a Spider Fibroin Gene Family

Paul A. Guerette, David G. Ginzinger, Bernhard H. F. Weber,* John M. Gosline†

Spiders produce a variety of silks that range from Lycra-like elastic fibers to Kevlar-like superfibers. A gene family from the spider *Araneus diadematus* was found to encode silk-forming proteins (fibroins) with different proportions of amorphous glycine-rich domains and crystal domains built from poly(alanine) and poly(glycine-alanine) repeat motifs. Spiders produce silks of different composition by gland-specific expression of this gene family, which allows for a range of mechanical properties according to the crystal-forming potential of the constituent fibroins. These principles of fiber property control may be important in the development of genetically engineered structural proteins.

Individual spiders generate up to seven mechanically distinct silk fibers by drawing liquid-crystalline proteins (*1*) from separate gland-spinneret complexes (*2*), but it is not known how spiders modulate the mechanical properties of silks. Silks are macromolecular composites of amorphous protein domains that are cross-linked and reinforced by β-sheet microcrystals; the degree of crystalline cross-linking and reinforcement largely determines functionally important mechanical properties (*3*, *4*). For example, spider dragline silk, which forms the spider's safety line and the frame of its web, contains 20 to 30% crystal by volume (*4*, *5*), forming a fiber that is stiff (initial Young's modulus, 10 GPa), strong (tensile strength, 1.5 GPa), and tough (energy to break, 150 MJ m^{-3}) (*4*). Spider viscid silk, which forms the spiral, glue-coated, capture portion of the web, contains ≤5% crystal by volume (*6*) and is mechanically similar to a lightly cross-linked rubber, with low stiffness (initial Young's modulus, 3 MPa) and high extensibility (*4*).

Factors that influence the formation and size of the crystals include the primary and secondary structure of the proteins, control of the genes that encode these proteins, and the chemical and mechanical processing of the proteins during spinning. X-ray diffraction studies on silks and synthetic polypeptides indicate that the amino acid sequence motifs that form β-sheet crystal domains are either poly(alanine) repeats (for example, spider silk) (*4*, *5*, *7*) or repeat motifs where glycine alternates with either alanine or serine (for example, the GAGAGS repeat in *Bombyx mori* cocoon silk) (*8*, *9*). In addition, a large fraction of the protein in silk appears noncrystalline or "amorphous" by x-ray diffraction (*8*), and therefore other sequence motifs may direct the organization of amorphous domains. In the fibroins of the spider *Nephila clavipes*, the crystal-forming poly(alanine) blocks are separated by glycine-rich domains that are similar to the β turn–forming motifs in elastomeric proteins (*10*). We will refer to these as amorphous domains, although they may contain a degree of local order.

To investigate the control of crystallinity in silks, we examined the amino acid sequences of the silk proteins from the orb-weaving spider *Araneus diadematus*. Complementary DNA (cDNA) libraries were constructed from the major ampullate gland (MA; dragline silk), the flagelliform gland (FL; viscid silk), and the cylindrical gland (CY; cocoon silk) (*11*). These libraries were screened with probes that were based on the previously cloned spidroin-1 and spidroin-2 from the spider *N. clavipes* (*12*), hereafter called NCF-1 and NCF-2. Four distinct, partial silk cDNAs were isolated, each of which contained silklike protein repeat motifs, 78 to 101 residues of a nonsilk COOH-terminal protein domain, and a unique 3′ untranslated region (UTR). The silklike protein repeats of the four cDNAs are shown in Fig. 1 and are named ADF-1 through ADF-4 (ADF, *A. diadematus* fibroin).

Of the silklike protein encoded by the

P. A. Guerette and J. M. Gosline, Department of Zoology, University of British Columbia, 6270 University Boulevard, Vancouver, British Columbia V6T 1Z4, Canada.
D. G. Ginzinger and B. H. F. Weber, Department of Medical Genetics, University of British Columbia, 2125 East Mall, Vancouver, British Columbia V6T 1Z4, Canada.

*Present address: Molekulare Humangenetik, University of Würzburg, D-97074 Würzburg, Germany.
†To whom correspondence should be addressed.

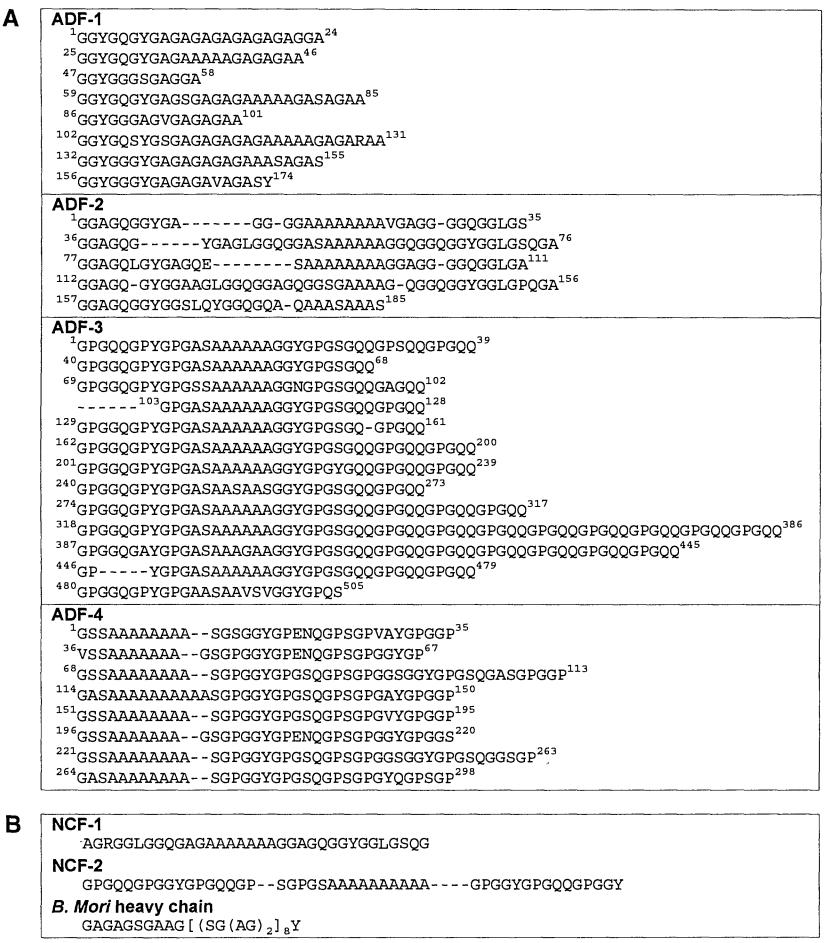

Fig. 1. (**A**) Predicted amino acid sequence in silklike regions encoded by four *A. diadematus* fibroin genes (*9*). The full, silklike sequence from partial cDNAs is arranged to align crystal and amorphous regions and to reveal the characteristic repeat motif of each protein. These repeat motifs are reiterated consecutively throughout the known predicted protein sequence up to 78 to 101 residues before the stop codon. (**B**) Consensus sequences from NCF-1, NCF-2, and *B. mori* heavy chain fibroin. Nucleotide and protein sequence data have been deposited in GenBank (accession numbers U47853 to U47856).

ADF-1 clone, 68% is present as poly(alanine) blocks five residues long, or as $(GA)_n$ blocks (n = 2 to 7); these motifs are known to form β-sheet crystals (*8*). The remaining 32% is occupied by GGYGQGY repeats (*9*), and predictors of secondary structure suggest that these are noncrystalline (*13*). ADF-2 encodes crystal-forming poly(alanine) blocks ~8 residues long (19%); the remainder (81%) is formed from GGAGQGGY and GGQGGQ-GGYGGLGSQGA repeats, which are similar to sequences in elastin and lamprin (*10*, *14*). Repeats of this type likely contribute to the noncrystalline scattering seen in x-ray diffraction patterns of elastic proteins and silks. ADF-3 and ADF-4 proteins are distinct because they are rich in proline. ADF-3 encodes crystal-forming ASAAAAAA blocks (21%) and amorphous repeat blocks (79%) of GPGGQG-PYGPG, GGYGPGS, and $(GPGQQ)_n$ (n = 1 to 8). ADF-4 contains crystal-forming SSAAAAAAAA blocks (27%) and amorphous repeat blocks of GPGSQGPS and GPGGY (73%).

There are strong similarities between the four genes cloned in this study and the genes that encode NCF-1 and NCF-2, and we suggest that they are part of the same gene family. All of these genes encode proteins that exhibit the pattern of alternating alanine-rich, crystal-forming blocks and glycine-rich amorphous blocks that are similar in size. In addition, the COOH-terminal domains of all spider fibroins show strong identity, and they contain a highly conserved cysteine residue (Fig. 2A, bold) that may participate in interfibroin disulfide cross-linking (*15*). This domain shows 40 to 91% strict identity and 63 to 95% functional identity (Fig. 2B). The very high identity (95%) between the ADF-3 and *A. bicentenareus* fibroin (ABF-1) suggests that these two are species-specific variants of a single gene. ADF-1 is the most distinct of all the spider fibroins in both crystal and amorphous repeat motifs, and it shows lowest identity to other *Araneus* and *Nephila* fibroins. It is not clear whether the proteins from *Nephila* are species-specific variants of *Araneus* fibroins or are additional members of the gene family, and it will not be possible to resolve this issue without COOH-terminal sequence data from related spiders.

Although the proteins encoded by this gene family are similar, the variation in the silklike domains is sufficient for differential gene expression to provide the potential for modulating the crystallinity, and hence the mechanical properties, of a specific silk type. Northern (RNA) blots containing total RNA from all seven silk glands from *A. diadematus* were probed with 3′ restriction fragments from each of the four ADF cDNAs (*16*), and they showed gland-specific expression of all four silk genes. The ADF-1 transcript (8.5 to 9.5 kb) is expressed in very large amounts in the minor ampullate (MI) gland (Fig. 3A), and the predicted

A

```
                                0        10        20        30        40        50        60        70        80
ADF-1          175GGA-VRLSSAGAAS- RVSSNVAAIA SAG---AAAL PNVISNIYSG V-LS-SGVSS SEALIQALLE VISALIHVLG SASIGNVSSV GVN-SALNAV Q262
ADF-2                186RLSPS-AA-- RVSSAVSSLV NGGPTSPAAL SSSISNVVSQ ISASNPGLSG CDILVQALLE IISALVHILG SANIGPVNSS SAGQSASIVG QSVYRALS281
ADF-3      506SSVPVASAVASRLS-SPAASS RVSSAVSSLV SSGPTKHAAL SNTISSVVSQ VSASNPGLSG CDVLVQALLE VVSALVSILG SSSIGQINYG ASAQYTQMVG QSVAQALA613
ADF-4    299GAYGPSPSASVAASVYLRLQPRL EVSSAVSSLV SSGPTNGAAV SGALNSLVSQ ISASNPGLSG CDALVQALLE LVSALVAILS SASIGQVNVS SVSQSTQMIS QALS405
NCF-1                            RVSSAVSNLV ASGPTNSAAL SSTISNVVSQ IGASNPGLSG CDVLIQALLE IVSALIQILG SSSIGQVNYG SAGQATQI
NCF-2                            RVASAVSNLV SSGPTSSAAL SSVISNAVSQ IGASNPGLSG CDVLIQALLE IVSACVTILS SSSIGQVNYG AASQFAQV
ABF-1                            RVSSAVSSLV SSGPTTPAAL SNTISSAVSQ ISASNPGLSG CDVLVQALLE VVSALVHILG SSSVGQINYG ASAQYAQM
                                 ******* **   ***  *** * **  ***   ******** ** * ******.  ***  *** * ***  *      *
```

B

	ADF-1	ADF-2	ADF-3	ADF-4	NCF-1	NCF-2	ABF-1
ADF-1	–	69	63	65	63	65	65
ADF-2	*47*	–	81	83	85	79	86
ADF-3	*44*	*68*	–	82	87	85	95
ADF-4	*40*	*68*	*72*	–	82	82	82
NCF-1	*44*	*74*	*78*	*70*	–	87	87
NCF-2	*42*	*69*	*73*	*67*	*81*	–	86
ABF-1	*44*	*71*	*91*	*71*	*74*	*76*	–

Fig. 2. COOH-terminal domain identity for spider fibroins. (**A**) The COOH-terminal amino acid sequences of ADF-1 through ADF-4, NCF-1, NCF-2, and ABF-1 (*18*) are aligned and compared. Asterisks denote amino acids that are conserved in at least six of the seven sequences (*9*). The conserved cysteines are shown in bold type. (**B**) Percent identity matrix for the first 78 residues of the COOH-terminal domains. The values in italics denote strict identity; the remainder show functional identity with conservative amino acid substitutions.

amino acid composition of the encoded silklike repeat is virtually identical to that of the accessory fiber (MI, Table 1). Thus, ADF-1 is a major constituent of the MI silk, and it is likely that the sequence motif in the partial cDNA is representative of the entire gene. Bands at ~8.5 and ~9.5 kb (Fig. 3F) represent possible splicing variants of ADF-1 or cross-hybridization to closely related family members.

Moderately large amounts of ADF-2 transcript are found in the CY gland, with three doublets at ~8, ~12, and ~14 kb (Fig. 3B). Thus, ADF-2 is likely a constituent of cocoon silk, but because its predicted amino acid composition is quite different from that reported for this silk (CY, Table 1), we believe that other unidentified proteins must also be present. The multiplicity of bands likely indicates cross-hybridization to closely related, as yet unidentified, CY-specific fibroin genes.

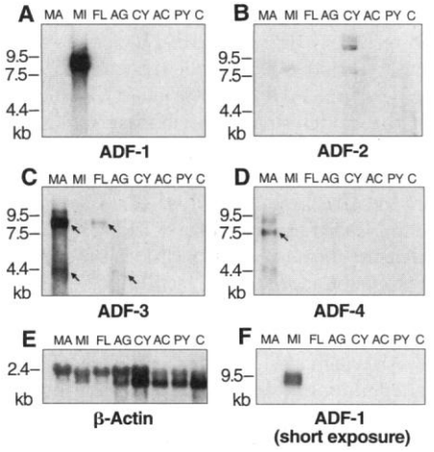

Fig. 3. Northern blot analysis of silk gland distribution of (**A**) ADF-1, (**B**) ADF-2, (**C**) ADF-3, (**D**) ADF-4, (**E**) β-actin control, and (**F**) ADF-1 (short exposure). Lanes: MA, major ampullate gland (dragline silk); MI, minor ampullate gland (accessory fiber); FL, flagelliform gland (viscid silk); AG, aggregate gland (viscid glue); CY, cylindrical gland (cocoon silk); AC, aciniform gland (swathing silk); PY, pyriform gland (attachment silk); and C, control spider visceral tissue. All lanes contained similar amounts of RNA, as verified with the β-actin control.

ADF-3 shows very large transcript amounts (Fig. 3C) in the MA gland (~9.0 and ~4.4 kb; arrows) and modest amounts in the FL gland (~9.0 kb; arrow) and aggregate (AG) gland (~4.4 kb; arrow). A unique 21-base oligonucleotide from ADF-3 was used as a probe to confirm that the bands at ~9.0 and ~4.4 kb were specific to ADF-3 alone. This finding suggests either the presence of a splicing variant of ADF-3 or very similar heavy and light chain fibroin forms. ADF-4 is expressed in large amounts only in the MA gland (~7.5 kb; Fig. 3D, arrow). The bands at ~9.0 and ~4.4 kb are believed to represent cross-hybridization to the related ADF-3 transcript.

Our results indicate that MA silk (dragline) has at least two major protein constituents, both of which are rich in proline. These two proteins have similar glycine, alanine, and proline contents, but they differ in serine and glutamine content (Table 1). Interestingly, a 3:2 ratio of these two proteins would have an amino acid composition that is virtually identical to that of *A. diadematus* dragline (MA, Table 1). The amino acid composition of ADF-3 fails to account for the composition of the viscid silk (FL, Table 1), and therefore other viscid silk proteins remain to be cloned.

If spider fibroins, like virtually all other fibrous proteins, contain structural motifs that are repeated along the full length of the protein, then our analysis provides complete information on the major protein constituents of the MA and MI silks and partial information on the FL, CY, and AG silks. The four ADF probes hybridized weakly in several glands, and ADF-2, -3, and -4 were isolated from all three cDNA libraries; this finding indicates that in addition to the major patterns described above, small amounts of expression can occur. Finally, the lack of information on pyriform and aciniform silks indicates that the fibroin gene family contains other members and that much remains to be learned about spider silk genetics.

The properties of spider silks are determined in part by protein composition and in part during fiber spinning. Our results indicate that gene transcriptional control plays a major role in determining mechanical properties by controlling the potential for crystal formation. Thus, it should be possible to express and spin a battery of silk-based block copolymers with specifically tailored material properties by varying the proportion of crystal and amorphous coding domains in chimeric gene constructs.

Table 1. Percent amino acid composition of silklike repeats from ADF-1 through ADF-4 and four *A. diadematus* silks (*19*).

Amino acid	ADF-1	ADF-2	ADF-3	ADF-4	MA	MI	FL	CY
Glycine	46	47	38	34	37	43	44	9
Alanine	37	27	17	22	18	37	8	24
Serine	5	4	6	17	7	5	3	28
Proline	0	1	15	16	16	0	21	1
Glutamine	2	11	18	3	11	2	3	8
Tyrosine	9	4	5	5	4	5	3	1
Arginine	1	0	0	0	1	2	1	1
Valine	1	1	1	1	1	2	7	6
Leucine	0	4	0	0	1	1	1	6
Aspartate	0	0	0	1	1	2	3	6

REFERENCES AND NOTES

1. K. Kerkam *et al., Nature* **349**, 596 (1991).
2. F. Vollrath, *Sci. Am.* **266**, 70 (March 1992); J. M. Gosline, M. E. DeMont, M. W. Denny, *Endeavour* **10**, 37 (1986).
3. M. Denny, in *The Mechanical Properties of Biological Materials,* J. F. V. Vincent and J. D. Currey, Eds. (Cambridge Univ. Press, Cambridge, 1980), pp. 475–559.
4. J. M. Gosline *et al.,* in *Biomimetics,* M. Sarikaya and I. Aksay, Eds. (AIP Press, Woodberry, NY, 1995), pp. 237–261.
5. A. H. Simmons, C. A. Michal, L. W. Jelinski, *Science* **271**, 84 (1996).
6. J. M. Gosline *et al.,* in *Material Science and Biotechnology,* D. Kaplan, W. Adams, B. Farmer, C. Viney, Eds. (American Chemical Society, Washington, DC, 1994), pp. 328–341.
7. M. B. Hinman, S. L. Stauffer, R. V. Lewis, *ibid.,* pp. 222–233.
8. R. D. B. Fraser and T. P. MacRae, *Conformation in Fibrous Proteins* (Academic Press, New York, 1972).
9. Abbreviations for the amino acid residues are as follows: A, Ala; C, Cys; D, Asp; E, Glu; F, Phe; G, Gly; H, His; I, Ile; K, Lys; L, Leu; M, Met; N, Asn; P, Pro; Q, Gln; R, Arg; S, Ser; T, Thr; V, Val; W, Trp; and Y, Tyr.
10. J. Rosenbloom, W. R. Abrams, R. Mecham, *FASEB J.* **7**, 1208 (1993).
11. Complementary DNA libraries from MA, FL, and CY glands were generated with Stratagene's ZAP-cDNA synthesis kit and 5 μg of polyadenylated [poly(A)$^+$] RNA from 100 silk glands with the Micro-Fast Track mRNA isolation kit (Invitrogen). DNAs were ligated into the UNI-ZAP XR vector and packaged and propagated in Gigapack II Gold phage. Libraries were screened to the tertiary level at low stringency (42°C) with three oligonucleotide probes random-labeled with [α-^{32}P]deoxycytidine 5′-triphosphate (dCTP): 5′-GCAGCAGCAGCAGCAG-CA-3′, 5′-GGACAAGGAGGATATGGAGGT-3′, and 5′-GGACCAGGACAACAAGGACCAGGA-3′. Twenty putative silk clones were chosen from each library, and pBluescript phagemids with cDNA inserts were excised in vivo into *Escherichia coli* SOLR cells with the filamentous Exassist helper phage (Stratagene). Four unique partial cDNAs (ADF-1, 1.2 kb; ADF-2, 1.0 kb; ADF-3, 2.0 kb; and ADF-4, 1.4 kb) were sequenced from nested deletions generated with the Erase-A-Base system (Promega).
12. R. V. Lewis, *Acc. Chem. Res.* **25**, 392 (1992).
13. Mac Vector, version 4.1.1 (International Biotechnologies, New Haven, CT).
14. P. Robson *et al., J Biol. Chem.* **268**, 1440 (1993).
15. C. Jackson and J. P. O'Brien, *Macromolecules* **28**, 5975 (1995).
16. Total RNA was extracted from each tissue type (*17*), and 13 ± 3 μg per lane was electrophoresed, blotted, hybridized, and washed at high stringency according to standard methods. Blots were autoradiographed for 24 hours at −70°C. Blots were stripped and exposed for 3 days to ensure complete removal of previous probes before reprobing. Probes were obtained from low-melt restriction fragments of the 3′-most 180 to 250 nucleotides from each ADF cDNA and were random hexamer–labeled with [α-^{32}P]dCTP. These regions included the "unique" UTR sequence to minimize cross-hybridization to related transcripts.
17. P. Chomczynski and N. Sacchi, *Anal. Biochem.* **162**, 156 (1987).
18. R. Beckwitt and S. Arcidiacono, *J. Biol. Chem.* **269**, 6661 (1994).

19. S. O. Anderson, *Comp. Biochem. Physiol.* **35**, 705 (1970).
20. Supported by grants from Natural Sciences and Engineering Research Council of Canada and E. I. DuPont de Nemours & Co. to J.M.G. We acknowledge lab space provided by M. Hayden and critical review of the manuscript by H. Brock, T. Grigliatti, M. Lillie, and D. Nelson.

2 November 1995; accepted 8 February 1996

Replication of HIV-1 in Dendritic Cell–Derived Syncytia at the Mucosal Surface of the Adenoid

Sarah S. Frankel,* Bruce M. Wenig,* Allen P. Burke, Poonam Mannan, Lester D. R. Thompson, Susan L. Abbondanzo, Ann M. Nelson, Melissa Pope, Ralph M. Steinman†

Human immunodeficiency virus–type 1 (HIV-1) replicates actively in infected individuals, yet cells with intracellular depots of viral protein are observed only infrequently. Many cells expressing the HIV-1 Gag protein were detected at the surface of the nasopharyngeal tonsil or adenoid. This infected mucosal surface contained T cells and dendritic cells, two cell types that together support HIV-1 replication in culture. The infected cells were multinucleated syncytia and expressed the S100 and p55 dendritic cell markers. Eleven of the 13 specimens analyzed were from donors who did not have symptoms of acquired immunodeficiency syndrome (AIDS). The interaction of dendritic cells and T cells in mucosa may support HIV-1 replication, even in subclinical stages of infection.

HIV-1 undergoes active replication in infected individuals even during periods of clinical well-being (*1*, *2*). It is important to identify sites of viral replication during the period of subclinical infection to understand pathogenesis and identify better therapies. Although lymph nodes are major reservoirs for extracellular virions, actively infected cells containing HIV-1 transcripts are infrequent and cells with intracellular viral protein are rare (*3*–*9*). Macrophages containing intracellular HIV-1 transcripts and Gag (p24) protein have been detected in the brains of infected individuals (*10*), but the specimens were from patients with terminal AIDS and the infected macrophages were present only in association with neurodegenerative changes that occur in some patients. The paucity of productively infected cells may mean that very few cells are responsible for viral replication in vivo or that active sites for HIV-1 replication have yet to be identified.

To investigate possible additional sites of virus replication, we examined specimens of adenoidal lymphoid tissue from 13 individuals, aged 20 to 42 years, two of whom were female. A detailed list of the patients is available on request. Each had undergone surgery between 1989 and 1995 to remove an enlarged adenoid, but the initial pathological analysis did not show changes associated with standard adenotonsillar infections or neoplasms. Further microscopic analysis at the Armed Forces Institute of Pathology revealed marked enlargement of the lymphoid follicles (B cell areas) and multinucleated giant cells. The latter are characteristic of chronic infections, but relevant organisms (tuberculous, fungal, parasitic, or viral) were not detected (*11*).

Within and just beneath the mucosa of the 13 specimens, cells were present that stained markedly for intracellular HIV-1 p24 antigen (*12*) (Fig. 1, B through E). The p24-positive cells either were large and irregularly shaped with a few nuclei or were "giant cells" with large numbers of nuclei and fewer dendrites. Weaker and diffuse staining for p24 was also observed in the underlying lymphoid follicles or germinal centers (Fig. 1B). The latter deposits likely represent extracellular antigen that was retained as antibody-coated virions on the surface of follicular dendritic cells (*3*, *6*, *8*, *13*). Infected cells were not detected in the adenoids of two HIV-1–negative controls (Fig. 1A). In situ hybridization with radio-

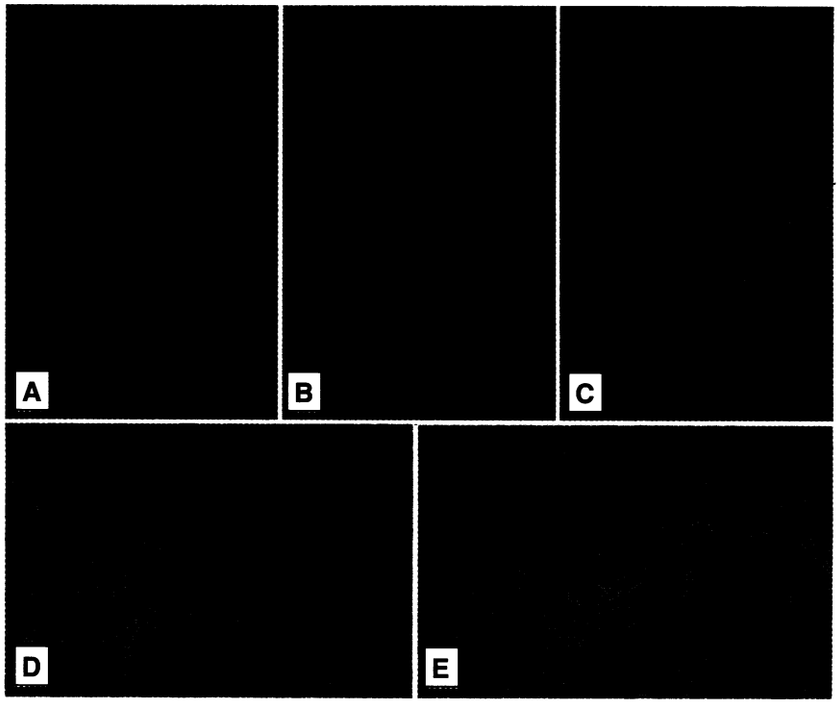

Fig. 1. Immunostaining of adenoidal lymphoid tissue for HIV-1 p24 protein. (**A**) Positive cells were not detected in the adenoid of uninfected individuals. Brackets indicate the mucosal epithelium that lines invaginations or plications of the surface (*). (**B** through **E**) Infected cells (brown) were present in and just beneath the mucosa (M) of all the HIV-1–positive specimens studied. Weak p24 staining in the germinal centers (GC) of the underlying lymphoid tissue is apparent in (B). HIV-1–infected syncytia, or multinucleated giant cells, are evident at higher magnification in (D) and (E).

S. S. Frankel and A. M. Nelson, AIDS Division, Department of Infectious and Parastic Disease Pathology, Armed Forces Institute of Pathology, Washington, DC 20306–6000, USA.
B. M. Wenig and L. D. R. Thompson, Department of Otolaryngic and Endocrine Pathology, Armed Forces Institute of Pathology, Washington, DC 20306–6000, USA.
A. P. Burke and P. Mannan, Department of Cardiovascular Pathology, Armed Forces Institute of Pathology, Washington, DC 20306–6000, USA.
S. L. Abbondanzo, Department of Hematologic and Lymphatic Pathology, Armed Forces Institute of Pathology, Washington, DC 20306–6000, USA.
M. Pope and R. M. Steinman, Laboratory of Cellular Physiology and Immunology, Rockefeller University, New York, NY 10021, USA.

*These authors contributed equally to this research.
†To whom correspondence should be addressed.